Acta Crystallographica Section B
Structural Science
ISSN 0108-7681

$[Ni(MeCN)(H_2O)_2(NO_3)_2]\cdot(15\text{-crown-5})\cdot MeCN$: detailed study of a four-phase sequence that includes an intermediate modulated phase

Maxime A. Siegler, Sean Parkin and Carolyn Pratt Brock*

Department of Chemistry, University of Kentucky, Lexington, KY 40506-0055, USA

Correspondence e-mail: cpbrock@uky.edu

Received 28 February 2012
Accepted 24 April 2012

A sequence of four phases has been found for an acetonitrile-solvated co-crystal with 15-crown-5 of the nickel complex [acetonitrilediaqua-κ^1O-nitrato-κ^2O-nitratonickel(II)]. The structure could be determined at intervals of *ca* 10 K in the range 90–273 K because crystals remain single through the three transitions. In phase (I) ($T \geq$ *ca* 240 K; $P2_1/m$, $Z' = \frac{1}{2}$), there is extensive disorder, which is mostly resolved in phase (III) (*ca* 230–145 K; $P2_1/c$, $Z' = 1$). Phase (IV) (*ca* 145–90 K, and probably below; $P\overline{1}$, $Z' = 2$) is ordered. Phase (II) (*ca* 238–232 K) is modulated, but the satellite reflections are too weak to allow the structure to be determined within its stability range by standard methods. Most crystals that were flash-cooled from room temperature to 90 K have a metastable $P2_1$, $Z' = 5$ superstructure that (at least in a commensurate approximation) was identified as similar to the structure of phase (II) by comparison of reconstructed reciprocal-lattice slices and by analogy with the phase behavior of the very similar compound $[Ni(H_2O)_6](NO_3)_2\cdot(15\text{-crown-5})\cdot 2H_2O$ [Siegler *et al.* (2011). *Acta Cryst.* B**67**, 486–498]. In the phase (II) structure slab-like regions that are like the disordered phase (I) structure alternate with regions of similar shape and size that are like the more ordered phase (III) structure.

1. Introduction

Crystals of $[Ni(MeCN)(H_2O)_2(NO_3)_2]\cdot(15\text{-crown-5})\cdot MeCN$ [acetonitrilediaqua-κ^1O-nitrato-κ^2O-nitratonickel(II) 15-crown-5 acetonitrile solvate; hereafter, Ni-MeCN] were obtained while we were working out how to make $[Ni(H_2O)_2(15\text{-crown-5})](NO_3)_2$ (Siegler *et al.*, 2008). The Ni-MeCN structure at 90 K has the refcode ROLCEB in the Cambridge Structural Database (hereafter the CSD; Allen, 2002). In the archived 90 K, $Z' = 2$ structure the monodentate (or, κ^1O) nitrato ligand has two different orientations (*ap* and *sp*; see Scheme 1) in the two independent Ni complexes.

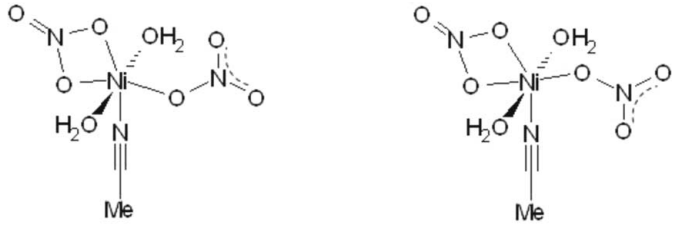

Scheme 1

At the time of the initial studies we discovered that the fully ordered ROLCEB phase could only be obtained by slow

cooling; crystals flash-cooled from room temperature to 90 K usually had a $Z' = 5$ structure analogous to the $Z' = 7$ structure found at 90 K for flash-cooled $[Ni(H_2O)_6](NO_3)_2\cdot$(15-crown-5)$\cdot 2H_2O$ (or NiW6-2W; see Siegler, Hao *et al.*, 2011). Since an investigation of NiW6-2W had revealed an unusual series of four phases we decided to look carefully at the temperature dependence of the Ni-MeCN structure. Again, we found an unusual series of four phases (see Fig. 1) that includes an intermediate phase with a large (or possibly incommensurate) unit cell.

The phases and their transition temperatures were identified by single-crystal X-ray diffraction methods. The phases were numbered from (I) (above *ca* 240 K) to (IV) (below *ca* 145 K). The lowest-temperature phase (IV) (ROLCEB; $Z' = 2$) is fully ordered. In phase (III) (*ca* 145–230 K; $Z' = 1$) the one independent κ^1O-nitrato ligand is disordered over the two orientations found in phase (IV); these two orientations (or conformations) are designated (see Scheme 1) as anti-periplanar (*ap*) and synperiplanar (*sp*) because the $N_{MeCN}-Ni-O_{mono}-N_{mono}$ torsion angle is either near 180° or less than 30°. In the highest-temperature phase (I) ($Z' = \frac{1}{2}$) the Ni complex is further disordered by a mirror plane that superimposes the bidentate (hereafter, κ^2O) and the disordered κ^1O nitrato ligands. Two atoms of the 15-crown-5 (hereafter, 15C5) molecule are also disordered by the mirror plane, but there is additional disorder of the 15C5 molecule that is not required by the mirror symmetry. Phase (II) (*ca* 232–238 K but studied at 90 K, where it is metastable) has a modulated structure ($Z' = 5$, at least in a commensurate approximation) in which some regions resemble phase (I) and others resemble phase (III).

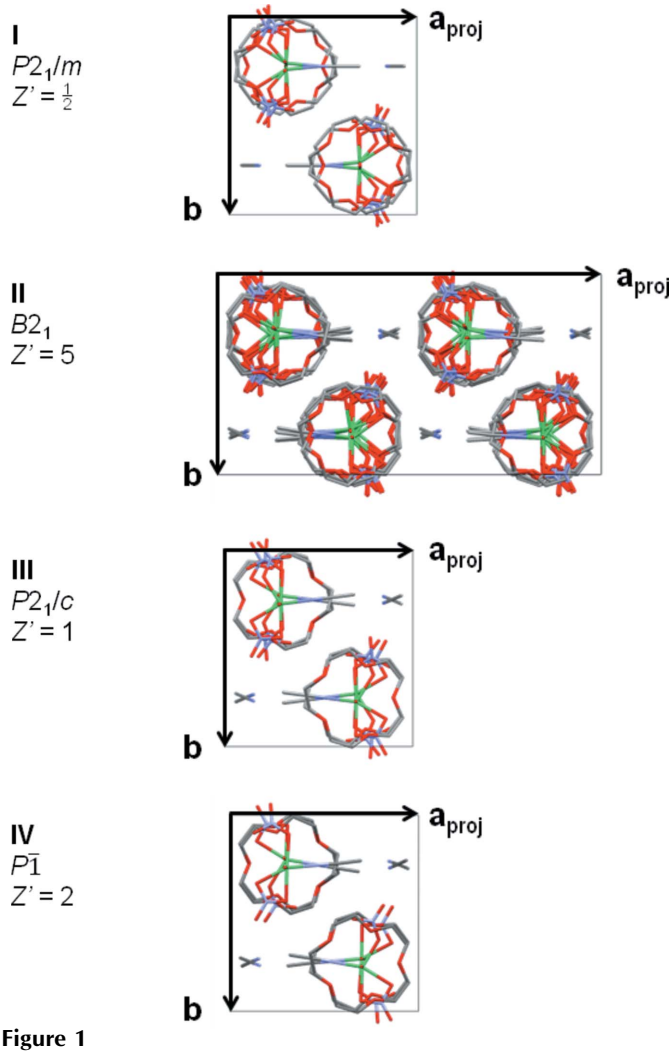

Figure 1
Diagram showing the four phases of $[Ni(MeCN)(H_2O)_2(NO_3)_2]\cdot$(15-crown-5)$\cdot$MeCN that were found between 273 K [phase (I)] and 90 K [phase (IV)]. All cells are shown in projection along **c**, which points into the drawing; the axes **a*** are in the plane of the drawing while the axes **a** point out of that plane. In the triclinic phase (IV) the axis **b** deviates from the plane of the drawing by no more than 0.06°. The relative lengths of the **c** axes are $c_I = c_{II}/5 = c_{III}/2 = c_{IV}/2$.

The primary packing feature of these structures is the hydrogen bonding between the 15C5 molecules and the $H_2O-Ni-OH_2$ unit of the Ni complex; the resulting $15C5\cdots H_2O-Ni-OH_2\cdots 15C5$ chains are very similar to those found in many related compounds (see Siegler *et al.*, 2008, 2010).

The compound described here and the NiW6-2W compound mentioned above (Siegler, Hao *et al.*, 2011) are two of the very few 'molecular' crystals that have been studied as a function of temperature through several phase transitions. For a list of the others archived in the CSD as of February 2010 see Table 1 in Siegler, Parkin *et al.* (2011).

2. Experimental

Pale green crystals of Ni-MeCN were obtained (Siegler *et al.*, 2008) by slow evaporation at room temperature of MeCN solutions equimolar in $Ni(NO_3)_2\cdot 6H_2O$ and 15C5. The crystals grew as irregular blocks elongated along **c**, which is the direction of the hydrogen-bonded chains. Not all attempts yielded crystals of acceptable quality; furthermore, attempts to reproduce the synthesis often led to crystals of the first polymorph of $[Ni(H_2O)_6](NO_3)_2\cdot$(15C5)$\cdot H_2O$ and of *cis*-$[Ni(H_2O)_4(NO_3)_2]\cdot$*trans*-$[Ni(H_2O)_4(NO_3)_2]\cdot 2$(15C5) (see Siegler *et al.*, 2008) rather than to crystals of the desired Ni-MeCN compound.

2.1. Differential scanning calorimetry (DSC)

DSC measurements were performed using the *DSC 822^e* apparatus and the controlling software *STARe* (Version 8.10) manufactured by *METTLER TOLEDO*. The DSC samples were prepared from fine powders contained in aluminum crucibles. The amount of powdered sample was 3.89 mg; heating and cooling rates were 5 and 10 K min^{-1} (two cycles each) in the range 143–243 K. The DSC traces (Fig. 2) were found to be less informative than the single-crystal X-ray experiments. Only one solid–solid phase transition was observed (*ca* 215–220 K), and the associated heat change was so small that no reliable value of $\Delta_{tr}H$ could be determined. Instrumental limitations prevented measurements below 143 K so that there was little chance of observing the transition (III) ↔ (IV).

Table 1
Experimental details.

For all structures: $C_{10}H_{20}O_5{\cdot}C_2H_7N_3NiO_8{\cdot}C_2H_3N$, M_r = 521.13. Experiments were carried out with Mo $K\alpha$ radiation using a Nonius KappaCCD diffractometer. Absorption was corrected for by multi-scan methods, *SCALEPACK* (Otwinowski & Minor, 2006). H atoms were treated by a mixture of independent and constrained refinement.

	(I) at 243 K	(II) at 90 K	(III) at 230 K	(III) at 150 K	(IV) at 120 K
Crystal data					
Crystal system, space group	Monoclinic, $P2_1/m$	Monoclinic, $B2_1$	Monoclinic, $P2_1/c$	Monoclinic, $P2_1/c$	Triclinic, $P\bar{1}$
Temperature (K)	243	90	230	150	120
a, b, c (Å)	12.1311 (2), 12.3391 (2), 8.1432 (1)	27.4626 (4), 12.1845 (2), 40.2287 (6)	12.1589 (2), 12.2883 (2), 16.2261 (3)	12.1621 (2), 12.1890 (2), 16.0933 (2)	12.1535 (1), 12.1624 (1), 16.0614 (2)
α, β, γ (°)	90, 105.506 (1), 90	90, 122.026 (1), 90	90, 105.427 (1), 90	90, 105.451 (1), 90	90.036 (1), 105.464 (1), 90.026 (1)
V (Å^3)	1174.56 (3)	11412.5 (3)	2337.02 (7)	2299.51 (6)	2288.18 (4)
Z	2	20	4	4	4
μ (mm^{-1})	0.89	0.92	0.90	0.91	0.92
Crystal size (mm)	0.25 × 0.15 × 0.10	0.30 × 0.20 × 0.18	0.25 × 0.15 × 0.10	0.25 × 0.15 × 0.10	0.25 × 0.15 × 0.10
Data collection					
T_{min}, T_{max}	0.807, 0.916	0.770, 0.852	0.807, 0.916	0.804, 0.914	0.803, 0.914
No. of measured, independent and observed [$I > 2\sigma(I)$] reflections	5341, 2827, 1738	25 889, 25 889, 12 328	10 359, 5360, 3004	10 294, 5280, 3322	20 021, 10 485, 7796
R_{int}	0.033	0.085	0.045	0.049	0.040
Refinement					
$R[F^2 > 2\sigma(F^2)]$, $wR(F^2)$, S	0.041, 0.115, 1.02	0.058, 0.146, 1.11	0.074, 0.218, 1.36	0.043, 0.107, 0.98	0.044, 0.109, 1.13
No. of reflections	2827	25 889	5360	5280	10 485
No. of parameters	321	962	328	328	606
No. of restraints	151	1383	14	14	12
$\Delta\rho_{max}$, $\Delta\rho_{min}$ (e Å^{-3})	0.43, −0.25	0.70, −0.51	1.37, −0.56	0.84, −0.37	1.14, −0.53

Computer programs used: *COLLECT* (Nonius, 1999), *DENZO-SMN* (Nonius, 1999), *SHELXS*97 (Sheldrick, 2008), *SHELXL*97 (Sheldrick, 2008), *Mercury* (Macrae *et al.*, 2008), *SHELX*97 and local procedures.

2.2. Structure determinations

All X-ray data were collected with a Nonius KappaCCD diffractometer equipped with a CRYOCOOL-LN2 low-temperature system (CRYO Industries of America, Manchester, NH). Our calibrations of the CRYOCOOL-LN2 system using $N_2(l)$, the phase transition in $KH_2PO_4(s)$ near 122 K, and an $H_2O(s)/H_2O(l)$ bath indicate that the temperature precision is at least 0.2 K and the accuracy no worse than 0.5 K at the lowest temperatures, rising to about 1 and 2 K at room temperature. Mo $K\alpha$ radiation from a fine-focus sealed tube was used. In all cases the data in the unintegrated frames were transformed to reconstruct slices $nk\ell$, $hn\ell$ and hkn, n = 0–3, of the reciprocal lattice (hereafter RL slices). Sections of some RL slices illustrating the changes in the diffraction patterns through the phase transitions are included with the supplementary material.[1]

All structures were solved and refined in essentially the same way. The atom-numbering schemes (see Fig. 3) and the asymmetric units were kept as similar as possible to that of the original structure determination (ROLCEB). In structures having $Z' > 1$ the residue-numbering scheme available in *SHELXL* (Sheldrick, 2008) was used so that atom numbers

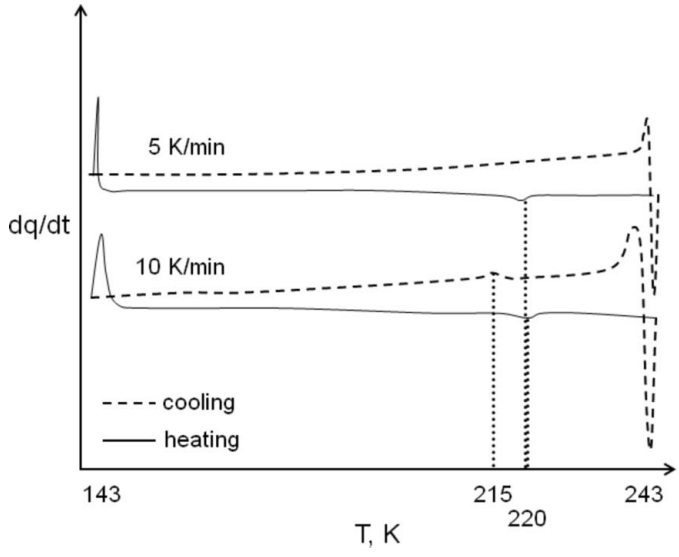

Figure 2
DSC traces for cooling/heating cycles measured at 5 and at 10 K min^{-1} for a typical sample of $[Ni(MeCN)(H_2O)_2(NO_3)_2]{\cdot}$(15-crown-5)·MeCN. Peaks for only one transition [phases (II) ↔ (III)] were found, and they are more obvious at the higher scan rate. The large peaks at the highest and lowest temperatures are instrumental artifacts. The temperature of the transition (III) ↔ (IV) (*ca* 145 K) was probably too low to be observed with the instrument used.

[1] Supplementary data for this paper are available from the IUCr electronic archives (Reference: HW5021). Services for accessing these data are described at the back of the journal.

would be the same in all formula units (*e.g.* O8_1 and O8_2 in the $Z' = 2$ structures). The H atoms of the 15C5 molecules were placed at calculated positions (*AFIX* 23) with U_{iso} values $1.2U_{eq}$ of the attached C atom. The H atoms of MeCN groups (U_{iso} values $1.5U_{eq}$ of the attached C atom) were placed at idealized positions (*AFIX* 137) with the rotation angle determined by the condition that the electron density at the atom sites be maximized. The H atoms of the water ligands were located in difference-Fourier maps and restrained such that the O—H distances and H—O—H angles had values within accepted ranges [target bond length 0.840 (1) Å and bond angle 104.5 (2)°]. The U_{iso} values were set at $1.5U_{eq}$ of the attached O atom. The weighting schemes were $w = [\sigma^2(F_o^2) + (W_1P)^2 + (W_2P)]^{-1}$, $P = (F_o^2 + 2F_c^2)/3$, where W_1 varied from 0.04 to 0.09 and W_2 was 0 except in the four highest temperature refinements for phase (IV), where W_2 was 0.40.

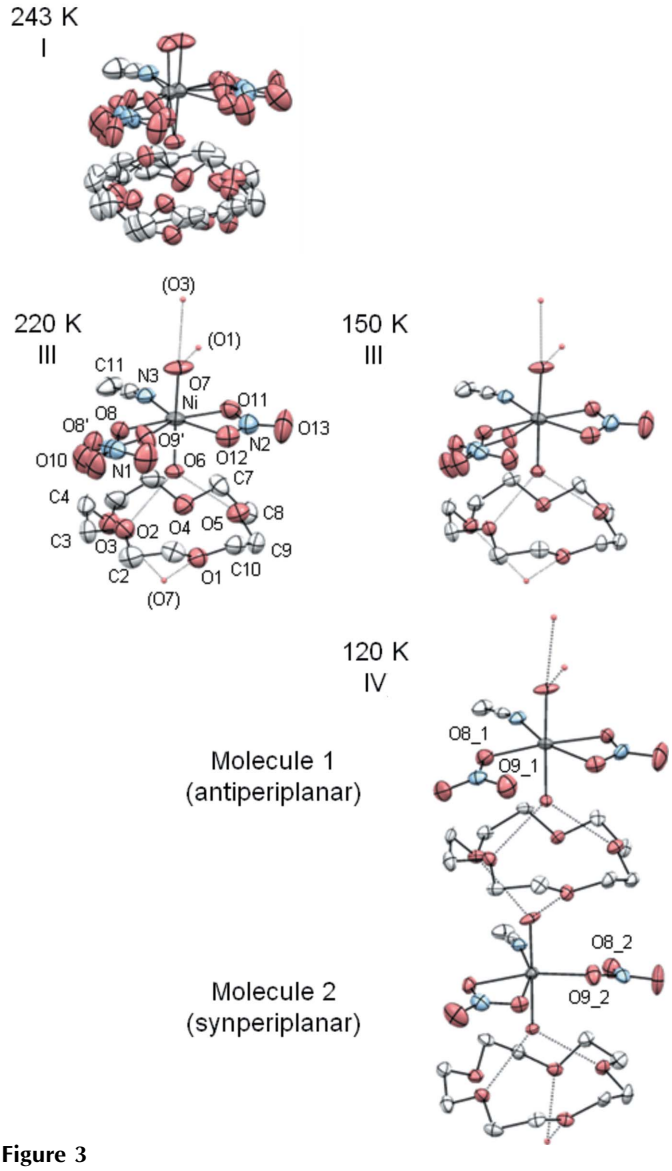

Figure 3
Ellipsoid plots (50% probability level) for the asymmetric unit (two formula units) of phase (I) at 243 K, of phase (III) at 220 and 150 K, and of phase (IV) at 120 K. The atom-numbering scheme is shown; the numbers of the atoms that are not labeled can be worked out from the labels given. The O—H···O bonds for phase (I) are not shown because of the extensive disorder.

Details of five structure determinations are presented in Table 1. Information about the other 23 determinations is available with the supplementary material.

2.2.1. Multi-temperature studies. Two crystals were studied as a function of temperature. The first crystal was cooled slowly (2 K min^{-1}) and then studied from 90 to 273 K in 17 steps of 10 K and one step of 13 K. The second crystal was also cooled slowly and was then studied from 210 to 243 K in eight steps of 3 K and one step each of 5 and 4 K. A full data set was collected at each temperature. In all cases there was a delay of at least 20 min between raising the temperature and starting data collection.

Initially the unit cell at each temperature was that picked by the software (Otwinowski & Minor, 2006) as the best choice for integrating the raw data frames. Because the satellite peaks in phase (II) are so weak in the regions where the phase is stable, this procedure led to phase (II)'s being integrated in the $P2_1/m$ cell of phase (I) (*i.e.* in the basic cell of the modulated structure). The presence of satellite peaks in the RL slices $hn\ell$, n = 1–3 was, however, obvious at 233 and 236 K, and possible at 239 K (see supplementary material). The temperatures of the phase transitions into and out of phase (II) were determined from the appearance and disappearance in the RL slices of these (unindexed) superstructure reflections.

2.2.2. Phase (IV). The refinements started from the coordinates of ROLCEB. The refinements of data measured to 130 K (*i.e.* to *ca* 15 K below the phase transition) were straightforward, although there are a few eccentric ellipsoids at 130 K. The structure is twinned by pseudomerohedry either about a twofold axis parallel to **b** or by a mirror plane perpendicular to **b**; the parameter describing the smaller volume fraction (Flack, 1983) increases from 0.451 (1) at 90 K to 0.463 (1) at 130 K. We saw no evidence of additional twinning even though the lengths *a* and *b* are very similar (see Table 1).

A plot (see Fig. 4) of the scaled intensities of the ten most intense $h0l$, $h + l$ odd reflections of phase (IV) indicates that the phase transition occurs between 140 and 150 K. Refinement of the 140 K data in the phase (IV) structure, however, led to three atomic displacement ellipsoids that are non-positive definite and to others in the κ^1O and κ^2O nitrato ligands that are very eccentric. We concluded that either the diffraction pattern measured at 140 K does not contain sufficient information about the deviations from the phase (III) structure to support refinement in the phase (IV) cell or that at 140 K domains of phases (III) and (IV) are both present. Examination of the peaks in the final difference Fourier map suggested (see below) that the latter explanation is the more likely. The results of this imperfect refinement are included in the supplementary material because we believe they are more informative than a more constrained (*e.g.* isotropic) refinement would be.

2.2.3. Phase (III). In phase (III) the one κ^1O nitrato ligand has two orientations (see Scheme 1 and Fig. 3). Restraints *FLAT* and *DANG* were imposed on that nitrate ion and *EADP* instructions were used to keep the displacement ellipsoids of the members of the nearly superimposed atom pairs N1/N1′ and O10/O10′ equal. Except at the extremes of the stability range the occupancy factors do not differ from 0.5 by more than two s.u.s, which are in the range 0.005–0.010. At the low end of the temperature range (150 and 160 K), however, the occupancy factors for the *ap* orientations are 0.479 (5) and 0.482 (5) for the first crystal studied at multiple temperatures and 0.475 (4) for yet another crystal cooled slowly to 150 K. At 230 K the occupancy factor for the *ap* orientation is 0.553 (14). It is possible that the occupancy factor depends weakly on temperature.

2.2.4. Phase (II). In the first multi-temperature sequence there is convincing evidence in the RL slices at 233 K for satellite reflections corresponding to a modulated cell but they are very weak. In the second multi-temperature sequence data for phase (II) were collected more slowly. At 230 K no extra peaks were seen, but new peaks were obvious at 233 and 236 K. The peaks are stronger at 233 than at 236 K, partly because the data were measured with a 50% longer exposure time. In the RL slices for the data collected at 239 K there is evidence of some extra, but quite diffuse, peaks (see supplementary material). On the other hand, the RL slices for a crystal studied earlier at 233 K after slow cooling (2 K min^{-1}) showed no indication of extra peaks. Hysteresis in the transition (I) ↔ (II) may explain the discrepancy.

Three crystals that were flash-cooled from room temperature to 90 K were all found to be in a metastable modulated phase that has, at least in a commensurate approximation, the space group $P2_1$ with $Z' = 5$. To facilitate comparisons with the

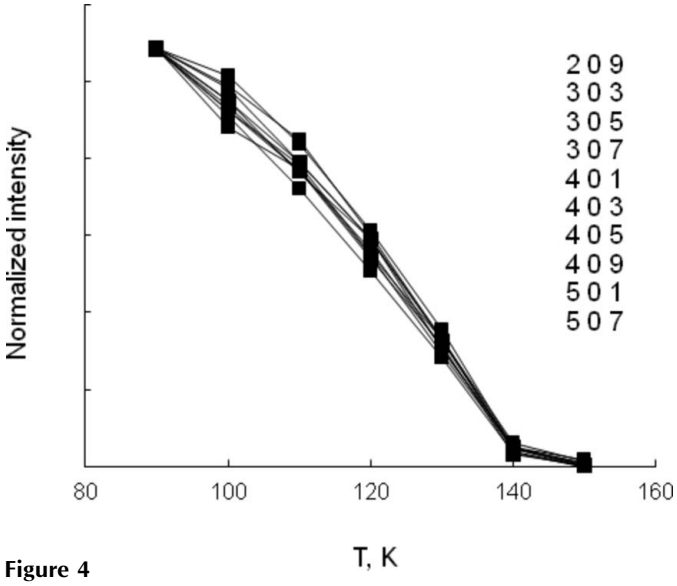

Figure 4
Temperature dependence of the integrated intensities of the 10 strongest *h*0*l*, *l* odd reflections of phase (IV) ($P\bar{1}$). The indices of these reflections are shown. After the transition to phase (III) ($P2_1/c$; nearly the same cell dimensions) these reflections are systematically absent. At 140 K the range of $I/\sigma(I)$ values is 3.7–12.0; at 150 K the range is 0.0–0.8, the transition must therefore take place between these two temperatures.

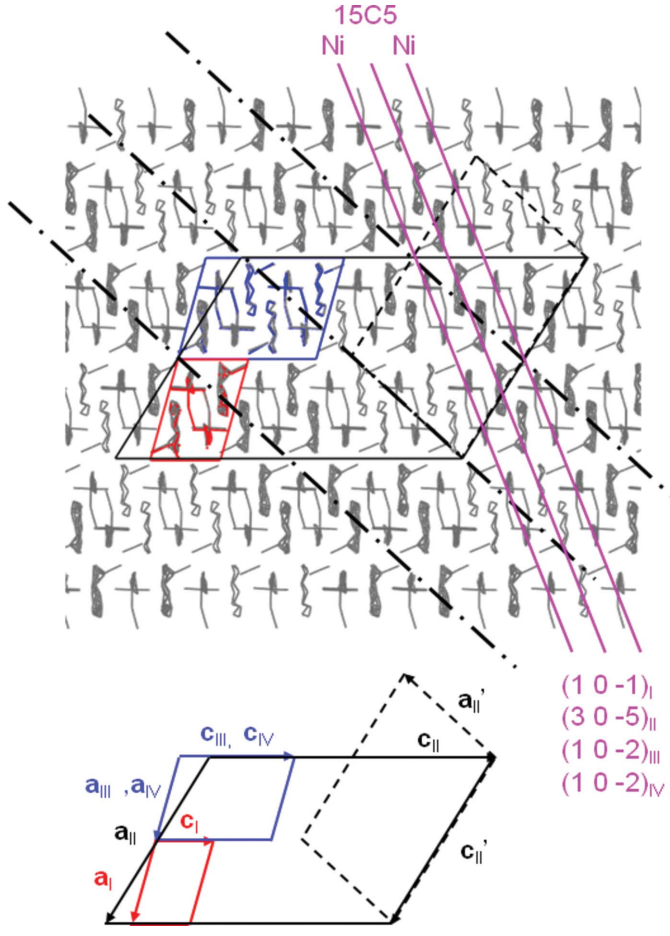

Figure 5
Overlay showing projections along **b** of the structures of phases (I)–(IV). The conventional $P2_1$ cell for phase (II) is shown with dashed lines; the axial labels for the $P2_1$ cell are primed. The $B2_1$ cell used is shown with solid black lines. The planes composed of Ni complexes and of 15-crown-5 molecules are marked with magenta lines; these planes are (1 0 $\bar{1}$) in phase (I), (1 0 $\bar{2}$) in phases (III) and (IV), and (3 0 $\bar{5}$) in phase (II). Three planes perpendicular to the apparent modulation vector are also marked (black broken lines); two of the planes marked pass through the most disordered regions of the structure and one passes through the most ordered region.

conventional unit cells of phases (III) and (IV) this $P2_1$ cell was transformed to a $B2_1$ cell so that the hydrogen-bonded chain (see Fig. 3) would be parallel to **c** (see Fig. 1). The transformation is **a**($B2_1$) = (0 0 1 / 0 1 0 / −2 0 −1) **a**($P2_1$), where the $P2_1$ cell dimensions are 17.326 (1), b = 12.184 (1), c = 27.463 (1) Å, and β = 100.19 (1)°. The reported structure (see Table 1) was refined in the $B2_1$ cell. The cell relationships are shown in Fig. 5.

Because the RL slices at 90 K strongly resemble the RL slices at 233 K (see Fig. 6 for a part of the *h*1*l* slice; see the supplementary material for comparisons of eight slices)[2] we

[2] Because the frames measured at 233 K had to be indexed in the $P2_1/m$ basic cell, and because only the axes **b** and **c** of the $B2_1$ and $P2_1/m$ cells are parallel (see Fig. 5), only the axes **a*** and **b*** of the $B2_1$ and $P2_1/m$ cells are parallel. The only RL slices that can then be compared directly are the *hkn* and *hnl* slices. In the *hkn* slices the axes **a*** and **b*** are parallel but n for the $B2_1$ cell must be 5× larger than n for the $P2_1/m$ cell. In the *hnl* slices the **a*** axes are parallel but the **c*** axes are not.

believe that the structure metastable at 90 K is very similar to the structure of phase (II) in its stability range (*ca* 232–238 K). The streaks seen at 90 K (see Fig. 6) but not observed at 233 K suggest, however, that the structure at 90 K that was refined conventionally is only an approximation. Those streaks are parallel to **a*** − **c*** of the $B2_1$ cell or to **c*** of the $P2_1$ cell (see Fig. 5). The RL slices *nkl*, *n* = 0–3, for the $P2_1$ cell (see supplementary material) show that there is no **b*** component to the streaks. Very similar results were obtained for a second flash-cooled crystal.

In the best set of data measured at 90 K for a phase (II) crystal, 47.6% of the reflections to $\sin\theta/\lambda = 0.65$ Å^{-1} have $I > 2\sigma(I)$; the $R_{\rm merge}$ value is 0.085. The corresponding structure is disordered in complicated ways but could be solved surprisingly easily and refined (with restraints) without difficulty (see Table 1). The Ni—O distances of the nitrato ligands were restrained to 2.05 (4) Å for κ^1O, and 2.12 (4) Å for κ^2O, coordination. In the nitrato ligands the N—O distances were restrained to 1.27 (4) Å for the O atom coordinated to Ni and to 1.22 (4) Å for the other two O atoms.[3] Planarity restraints (*FLAT* 0.005) were applied to all NO_3^- ions. *SAME* instructions were used to keep the distances and angles in the three sets of five independent molecules similar. Displacement parameters for the corresponding atoms in the five chemical units were set equal by the use of free variables; EADP instructions could not be used because the pseudoglide operations that relate the different units change the signs of the U^{12} and U^{23} parameters. The number of free variables needed was (32–1)*6 = 186 rather than 32*6 because the U^{ij} values for C5 and C6 were set equal because of the extra disorder that affects those atoms (see below). A total of 11 free variables were used as occupancy factors. Occupancy factors for the Ni and O7 atoms were tied to the occupancy factor for the κ^1O nitrato ligand to which the distances indicated chemical bonding.

A conservative weighting scheme $\{w = [\sigma^2(F_o^2) + (0.05P)^2]^{-1}$, where $P = (F_o^2 + 2F_c^2)/3\}$ was used. Convergence was not a problem; the most important correlation coefficients in the final cycle had values of +0.86 and −0.84. The structure was refined as an inversion twin [refined volume fraction 0.493 (18)]. The final agreement factors are satisfactory, the displacement ellipsoids look normal, and the final difference Fourier map showed no peak larger than 0.70 e Å^{-3}. The largest peaks were located near some O atoms of some nitrato ligands.

2.2.5. Phase (I). Above *ca* 240 K the satellite peaks of phase (II) are absent and the structure is best described in a $P2_1/m$ cell with $Z' = \frac{1}{2}$. We chose to transform the conventional reduced cell by switching the axes **a** and **c** so that the hydrogen-bonded chains would be parallel to **c** as in ROLCEB. The dimension *c* in the nonstandard $P2_1/m$ cell is then very nearly half as long as in phases (III) and (IV).

In phase (I) all three molecules of the formula unit conform to mirror symmetry. That symmetry requires the disorder of C5 and C6 in the 15C5 molecule because the preferred conformation of the crown molecule is not completely compatible with mirror symmetry. There is also a separate 2:1 disorder of the 15C5 ring [occupancy factor 0.667 (3) for the major component at 243 K] that corresponds approximately to a 180° rotation around the ring normal or to an inversion through the ring center. The nitrato ligands of the Ni complex are also very disordered; the mirror plane requires disorder of the κ^1O and κ^2O nitrato ligands, and, as in phase (III), each κ^1O ligand has two orientations [occupancy factors 0.280 (12)(*ap*) + 0.220 (12)(*sp*) = 0.5 at 243 K]. The Ni and O7 atoms are also disordered, which is to say that the O6—Ni—O7 unit has two orientations that are anchored by the same O6

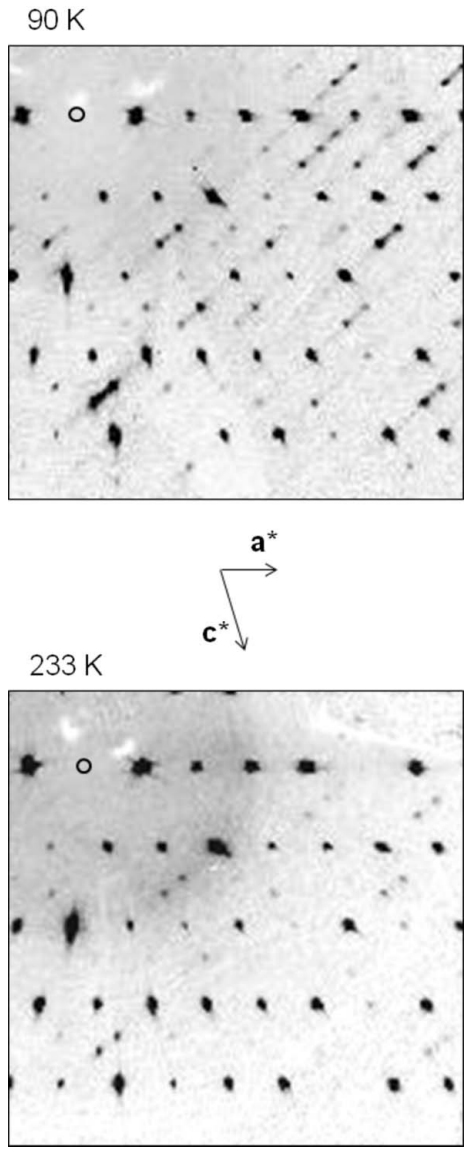

Figure 6
Part of the *h*1*l* reciprocal-lattice slice for phase (II) digitally reconstructed from the frames measured at 90 K, where the phase is metastable, and at 233 K. The origins (010 reflection) are marked, and the axes for the phase (I) ($P2_1/m$, $Z' = \frac{1}{2}$) cell are shown.

[3] Target distances were set by averaging the corresponding distances in the phase (IV) structure and then subtracting 0.01 Å because of the increased motion/disorder.

position. Any disorder of the ligand and lattice MeCN molecules has been absorbed into the displacement parameters, which are not, however, especially large or eccentric.

The refinement required many restraints. The C—C bond distances in the 15C5 molecule were restrained to 1.50 (2) Å and the C—O bond distances to 1.43 (2) Å. Displacement parameters for closely spaced atoms in the 15C5 molecules (*e.g.* C2 and C7′) and nitrato ligands (*e.g.* O10 and O10′) were set equal (*EADP* instructions). The N—O distances were restrained as they were in the phase (II) refinement, and a planarity restraint (*FLAT* 0.005) was applied to each of the two orientations of the κ^1O nitrato ligand. The refinement converged, but there were several large correlation coefficients (*e.g.* −0.98 for U^{22} and *y* of the Ni atom, and −0.93 for the *z* coordinates of C4 and C9′ of the 15C5 ring, which are separated by only 0.4 Å).

3. Results

3.1. Overview of the structures

The structures of the four phases are very similar. All have the same hydrogen-bonded chains in which 15C5 molecules and H_2O—Ni—OH_2 units alternate along the axis **c** (see Figs. 1 and 3). All phases have alternating, low-index layers (see Fig. 5) composed of either Ni complexes or 15C5 molecules (see Figs. 7 and 8). The lattice MeCN molecules bridge the two kinds of layers.

While data sets were collected as a function of increasing temperature we see no reason to suspect that the behavior would have been different (except for minor hysteresis) if data had been collected as a function of decreasing temperature.

3.2. Variation of cell dimensions with *T*

The transition from phase (IV) to (III) is not associated with any discernible discontinuity or change in slope of the cell dimensions with *T* (see Fig. 9). The changes associated with the transition from phase (III) at 230 K to (II) at 233 K are large enough to suggest a discontinuity. The transition (II) → (I) seems to be accompanied by changes in the slopes of the curves.

As *T* increases from 210 to 243 K *a* shortens. The direction of the greatest contraction is not actually along **a**, but is within 2.5° of being parallel to **a***, and is therefore nearly perpendicular to **b** and **c**. This direction is close to the horizontal direction of the drawings in Fig. 1.

3.3. Phase (I)

In the range 273–243 K the structure is best described by the space group $P2_1/m$ with $Z' = \frac{1}{2}$. Mirror symmetry is imposed on all three molecules. The symmetry requires that the C5 and C6 atoms of the 15C5 molecule be disordered because the preferred conformation of the molecule requires that those atoms lie on opposite sides of the mean molecular plane. The mirror planes also superimpose the κ^1O and κ^2O nitrato ligands of the Ni complex (see Figs. 3 and 7). The :NCMe ligand, the O6—Ni—O7 unit, and the included MeCN molecule must each either lie on a mirror plane or be disordered across it.

The coordinated and lattice MeCN molecules seem to be ordered, as does the water ligand containing O6; the displacement ellipsoids for these atoms do not seem to be especially elongated perpendicular to the mirror (see Fig. 3). The Ni atom and the O7 water ligand, however, are displaced to either side of the mirror.

There is further disorder that is not required by the space-group symmetry. Both the *ap* and *sp* orientations of the κ^1O nitrato ligand are present. There is also a 2:1 (see above) disorder of the 15C5 ring. We wondered if there might be at least some order in some directions (*e.g.* among molecules related by the 2_1 axes), but there are not any especially short

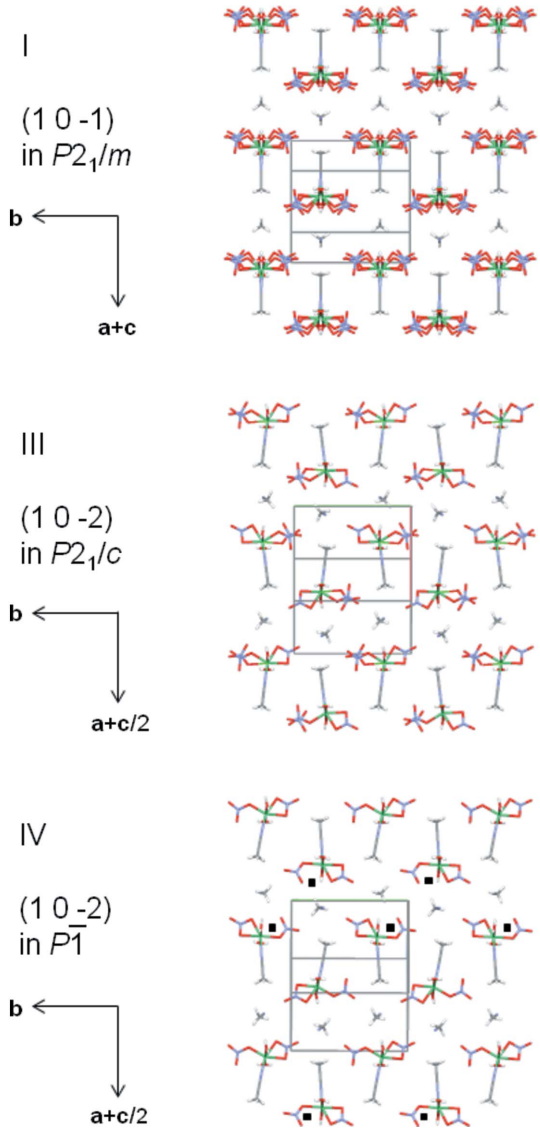

Figure 7
Diagram showing the layers containing the Ni complexes and the lattice MeCN molecules in phases (I), (III) and (IV). In the diagram for phase (IV) the complexes containing Ni_1 (*ap* conformation) are marked with filled squares. The methyl groups of the lattice MeCN molecules are closer to the mean plane than are their N atoms.

intermolecular contacts that would suggest local order. Furthermore, the difference between the occupancy factors for the two ring orientations (approximately 2:1) and for the κ^1O and κ^2O nitrato ligands (nearly 1:1) suggests that these two types of disorder are not strongly correlated. The packing in phase (I) seems to be quite loose.

We also failed to find any especially short contacts at 243 K [*i.e.* just above the transition to phase (II)] that would explain the structural changes that occur when the temperature is lowered. The $O_{Ni\_complex}—H\cdots O_{ether}$ contacts are important to the packing but they do not change much during the transition. There are C–H···N contacts between ligand and lattice MeCN molecules that are shorter than the sum of the

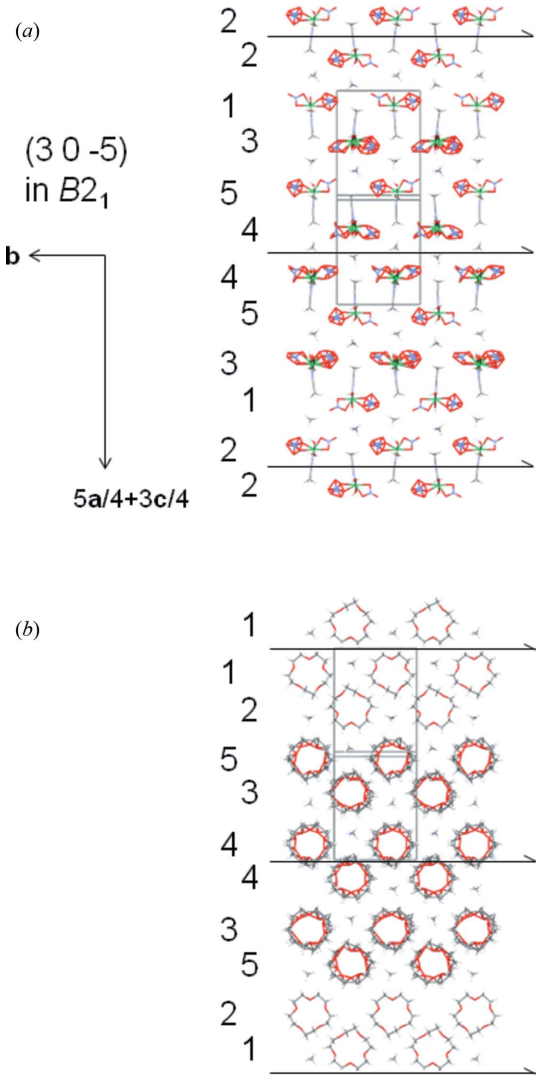

Figure 8
Diagram for the $B2_1$, $Z' = 5$ structure at 90 K showing the layers of (*a*) the Ni complexes, and (*b*) the 15-crown-5 rings. The lattice MeCN molecules bridge the two types of layers and so are shown in both; the methyl ends of the molecules are closer to the planes of the Ni complexes. The residue numbers of the Ni complexes and of the 15-crown-5 molecules are given for molecules in horizontal rows. In (*a*) the residue number of the lattice MeCN molecule is the same as that of the nearest Ni atom; in (*b*) the residue number of the lattice MeCN molecule is the same as that of the nearest O1 atom (which lies on an approximate mirror plane perpendicular to **b**).

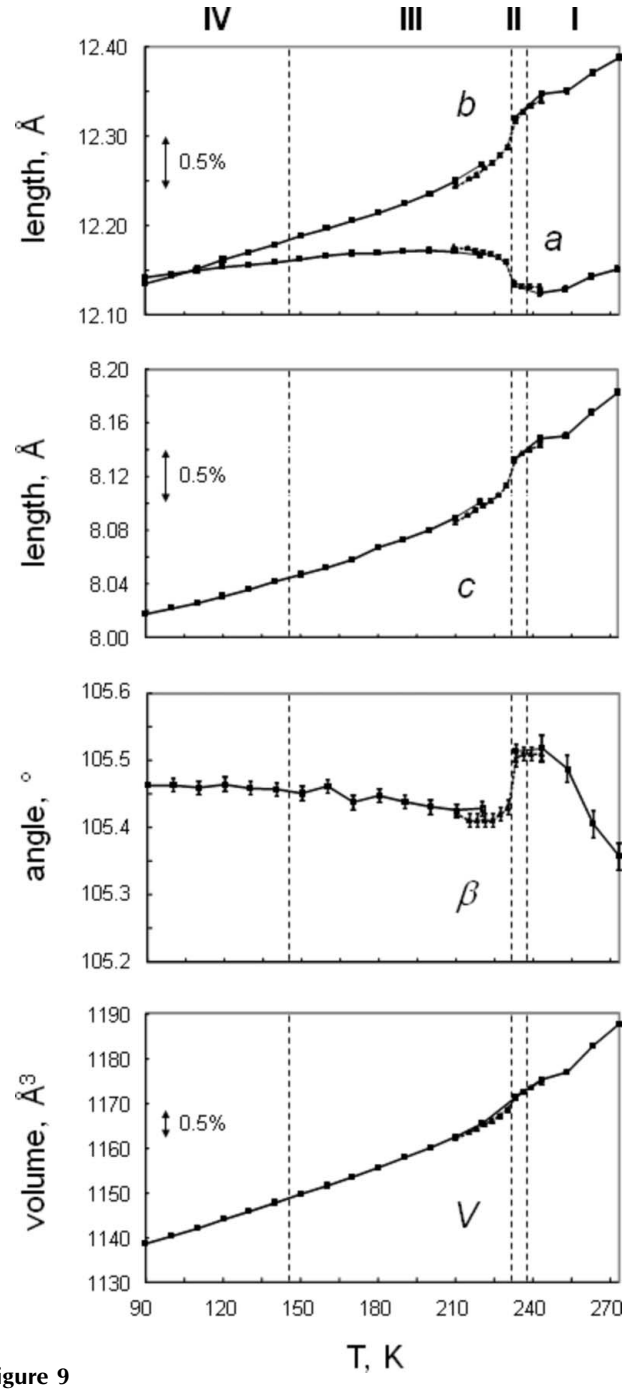

Figure 9
Temperature dependence of the cell dimensions of $[Ni(MeCN)(H_2O)_2(NO_3)_2]\cdot$(15-crown-5)·MeCN. The temperatures of the phase changes as determined during heating (see text) are marked by dashed lines. The unit cell for phase (II) is the $P2_1/m$ basic cell. The values of *c* for phases (III) and (IV) have been halved to bring all values to a common scale. The first crystal (square markers) was studied from 90–273 K in intervals of 10 K (except between 220 and 233 K). The second crystal (triangular markers) was studied in intervals of 3–5 K in the range 210–243 K. Estimated variabilities between crystals [±0.002 Å for *a* and *b*; ±0.001 Å for *c*; ±0.01° for β for phase (III)] are shown, but they are often smaller than the symbols used. Lines connect adjacent points. Note that the curves for *a* and *b* cross near 110 K so that at the lowest temperatures the triclinic cell used is not the reduced cell.

van der Waals radii (at least if the H atoms have been positioned correctly), and there are short C—H···O contacts, but it is not obvious that any of those contacts are structure determining.

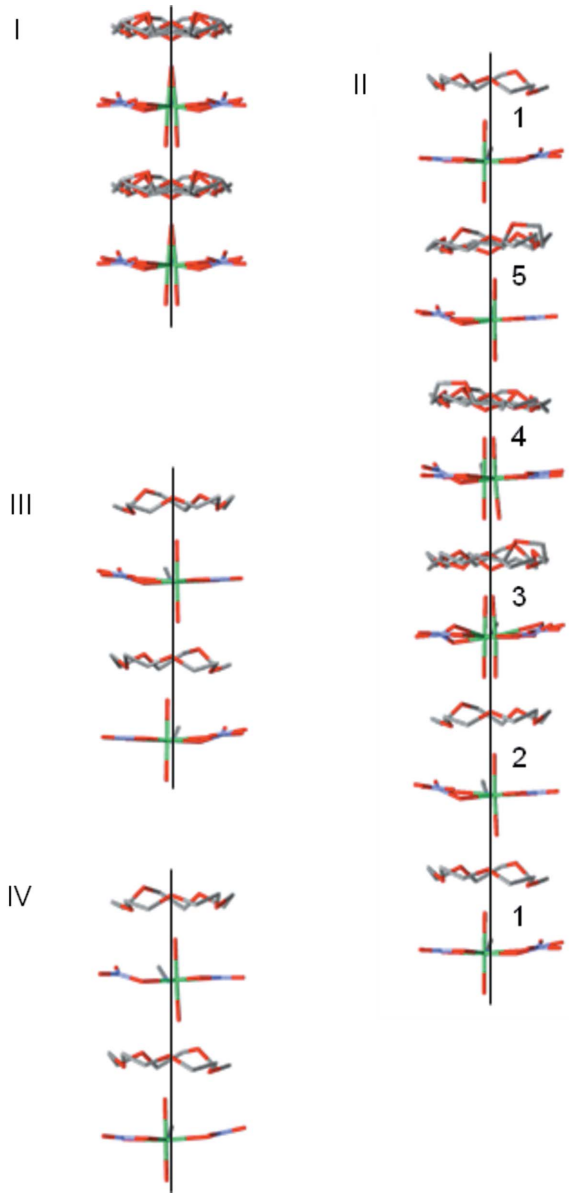

Figure 10
Segments of the hydrogen-bonded chains (hydrogen bonds not shown) in phases (I)–(IV). The axes **c** point vertically upwards; the axes **b** point from right to left. The two units shown for phase (I) (at 243 K) are related by translation; the two units shown for phase (III) (at 150 K) are related by the *c* glide. The two units shown for phase (IV) ($Z' = 2$) and five of the six units shown for phase (II) ($Z' = 5$) are symmetry independent (both structures at 90 K). The real [phase (I)] and approximate [phases (II)–(IV)] mirror planes are marked. The numbers shown for phase (II) are the residue numbers for the nearest Ni complex and 15-crown-5 molecule. The lattice MeCN molecules are not shown because they would be nearly superimposed on the H_2O—Ni—OH_2 units. The displacements of the Ni atoms along the horizontal axis **b** in phase (III) are ± 0.172, ± 0.199 and ± 0.205 Å at 230, 221 and 150 K. In phase (IV) these displacements are ± 0.258 Å at 140 K (where the structure is not well determined), ± 0.252 Å at 120 K, and ± 0.262 Å at 90 K.

3.4. Phase (III)

In phase (III) ($P2_1/c$ with $Z' = 1$; 230–150 K) most of the disorder found in phase (I) has been resolved. Loss of the mirror planes and doubling of the axis **c** allow small rotations of the Ni complexes (see Fig. 7) and ordering of the κ^2O nitrato ligands; these two changes lead to substantially denser packing along **b** (see Fig. 9). The disorder of the Ni atoms is cleared up so that there is an alternation of these atoms along **c**, *i.e.* along the hydrogen-bonded chains (see Fig. 10). In phase (III) the only remaining disorder is of the *ap* and *sp* orientations of the κ^1O nitrato ligand (see Figs. 3 and 7). Those two orientations need not have equal occupancy factors, but it seems (see above) that they probably do.

Superpositions of the eight phase (III) structures determined in the first multi-*T* sequence, and of the seven determined in the second, show only very minor changes with *T*. The displacement ellipsoids, except for those of the nearly superposed atom pairs N1/N1′ and O10/O10′, expand with temperature in a regular way.

At the lower end of the stability range the only important peaks in the final difference maps are at the midpoint of the Ni—O8 bond and approximately halfway between O9 and O12 (see Fig. 3). With increasing *T* the difference map becomes noisier. At *ca* 210 K and above the peak in the Ni—O8 bond persists, but the other major peaks strongly suggest at least minor disorder of the 15C5 ring resulting from an approximate twofold axis perpendicular to the ring plane as is found in phase (I).

3.5. Phase (IV)

During the transition (III) → (IV) the cell dimensions change only slightly but the screw axes and glide planes are lost ($P\overline{1}$, $Z' = 2$ below 150 K).[4] Strong pseudoglide symmetry remains, especially between the two independent 15C5 molecules. The deviations from the pseudoglide were estimated by calculating the distances between the corresponding atoms of the molecules 15C5_1 and 15C5_2 after taking the atoms of the latter through the transformation $x, -y + \frac{1}{2}, z + \frac{1}{2}$.[5] The maximum deviations along **a**, **b** and **c** for these atoms were found to be 0.06, 0.08 and 0.10 Å at 130 K and 0.07, 0.12 and 0.17 Å at 90 K.

The pseudosymmetry does not, however, relate the two κ^1O nitrato ligands. The Ni—O_{mono} bond in the complex containing Ni_1 (see Fig. 3) is to O8_1 (*ap* orientation); in the

[4] We find that during the transformation (III) → (IV) all the inversion centers are retained but that the glide planes and 2_1 screw axes are lost. The refined structures show that the only really significant change at the transformation is the resolution of the disorder in the monodentate nitrato ligand; the next largest change is in the positions of the MeCN molecules. Since the angles α and γ in phase (IV) deviate from 90° by less than 0.07° in phase (IV), and since the 0*k*0, *k* odd reflections are still unobserved, the possibility that the 2_1 axes are retained might seem a possibility. Such axes, however, would require that the Ni complexes they relate either all have the *ap* or all have the *sp* conformation. We find that the *ap* and *sp* conformations alternate (see Fig. 7). In projection down **b*** (see Fig. 5) the difference between the two conformations is minimal, which explains why the intensities of the 0*k*0, *k* odd reflections do not rise above the background.

[5] The transformation is nearly correct because the angles α and γ deviate from 90° by less than 0.1°.

other complex the bond is to O9_2 (*sp* orientation). The dihedral angles between the planes of the κ^1O and κ^2O nitrato ligands in the two complexes also differ between the two independent complexes; those angles vary from 9.9(*ap*) and 21.5°(*sp*) (Δ = 11.6°) at 140 K, to 13.0(*ap*) and 20.3°(*sp*) (Δ = 7.3°) at 130 K, and to 15.9(*ap*) and 19.0°(*sp*) (Δ = 3.1°) at 90 K

The angles α and γ of the triclinic cell increase monotonically from 90.008 and 89.990° at 140 K to 90.063 and 90.036° at 90 K (all uncertainties < 0.001°).

The four structures determined in the range 90–120 K are essentially superimposable; the displacement ellipsoids expand with T in a regular way. At 130 K (α = 90.025, γ = 90.007°), however, about half the ellipsoids for the eight atoms of the κ^1O nitrato ligands are too eccentric to correspond to any reasonable model of thermal motion. At 140 K three of the atoms in these ligands are non-positive definite and the ellipsoids of a few atoms in the κ^2O nitrato ligands look too small, too large, or too eccentric. There is no sign of trouble, however, in the ellipsoids for any of the other atoms in the structure.

The top ten residual peaks in all six structures determined at 90–140 K are all located in the planes of the nitrato ligands, with the highest peaks in the plane of the κ^1O NO_3^- ion. For the structures in the range 90–130 K the deepest hole is consistently in the range −0.48 to −0.56 e Å^{-3}. Since at 90 K there is only one peak higher than 0.55 e Å^{-3}, and it (at 0.65 e Å^{-3}) is located 0.97 Å from the Ni atom, we conclude that at 90 K the structure is ordered (R_1, wR_2 = 0.038, 0.088). As T rises the peaks larger than +0.60 e Å^{-3} all suggest the possibility of an alternate orientation of the κ^1O nitrato ligands very similar to that found in phase (III). At 120 K the four highest peaks (0.92–1.14 e Å^{-3}) are in the positions expected for atoms O8′_1, O9′_1, O8′_2, and O9′_2. At 130 and 140 K those peak heights are even greater (1.07–1.38 and 1.14–1.53 e Å^{-3}). At 140 K of R_1 and wR_2 are 0.054, 0.143.

It seems that when a crystal in phase (IV) is heated the κ^1O nitrato disorder found in phase (III) starts to appear at temperatures below that at which the $h0l$, $h + l$ odd reflections vanish and at which the angles α and γ become 90°. This nitrato disorder, however, has only very minor effects on the rest of the structure, which is still better described in $P\overline{1}$ with Z' = 2 rather than in $P2_1/c$ with Z' = 1. Careful inspection of the RL slices failed to turn up any indication of obvious non-Bragg scattering on either side of the transition (IV) → (III).

The unmodeled nitrato disorder could be random but is at least as likely to result from the presence of $P2_1/c$ domains in a crystal that consists primarily of $P\overline{1}$ domains. Attempts to determine possible contributions from two different phases that occur simultaneously will have to be part of a later project.

3.6. Phase (II)

The $B2_1$, Z' = 5 structure determined at 90 K is a complicated hybrid of the phase (I) and phase (III) structures. This hybrid structure is reminiscent of that found for the $B2_1$, Z' = 7 intermediate phase (commensurate approximation) of the related compound $[Ni(H_2O)_6](NO_3)_2\cdot$(15-crown-5)$\cdot 2H_2O$ (or NiW6-2W; Siegler, Hao *et al.*, 2011). An important lesson from that Z' = 7 structure, which could be refined at 213 K (the low end of its stability range) as well as at 90 K, is that occupancy factors determined at 90 K for a metastable version of a modulated phase may differ from those at a temperature where the phase is stable.

At 90 K the asymmetric unit of the Z' = 5 phase (in a commensurate approximation) includes [see Fig. 8(*b*)] two 15C5 molecules that were described as fully ordered and three that have two orientations with occupancy factors for the major component in the range 0.81–0.86 (s.u.s ≤ 0.003). Three of the Ni complexes (residues 1, 2 and 5) are like those of phase (III); there is no obvious disorder of the H_2O—Ni—OH_2 unit or involving the κ^2O nitrato ligands but there are two orientations of the κ^1O nitrato ligand. In the other two Ni complexes there is partial disorder of the H_2O—Ni—OH_2 units and the κ^1O/κ^2O ligands [occupancy factors 0.85 and 0.57 for the major components in residues 3 and 4, with s.u.s 0.003]. The range of occupancy factors for the two orientations of the κ^1O nitrato ligand in the five Ni complexes is 0.54–0.57 (residues 2–4) and 0.71–0.78 (residues 1 and 5; all s.u.s ≤ 0.005). Further details of the occupancy factors are given in the supplementary material.

The alternation pattern is not easy to understand because while the ordered complexes containing Ni_1 and Ni_2 are separated in the hydrogen-bonded chain by the ordered molecule 15C5_1, the ordered complexes containing Ni_5 and Ni_1 are separated by the disordered molecule 15C5_5. There is, however, a clear remnant of the phase (I) mirror (see Figs. 10 and 11), especially in the region of the lattice MeCN_4 molecule. Furthermore, the complex containing Ni_4, which is the complex nearest MeCN_4, has more complete κ^1O/κ^2O nitrato disorder [occupancy factors 0.573/0.427 (3)] than any of the other four Ni complexes. It is also worth remembering that the occupancy factors for the two 15C5 orientations in

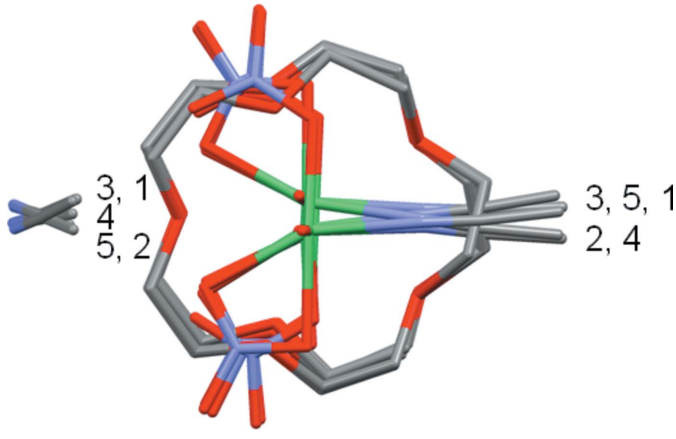

Figure 11
Projection down **c** of the five independent Ni complexes and five independent lattice MeCN molecules of phase (II) at 90 K. The Ni complex has two basic orientations. A remnant of the mirror symmetry of phase (I) is obvious in the orientation of the fourth lattice MeCN molecule. The disorder of the 15-crown-5 molecules and Ni complexes has been omitted for the sake of clarity.

phase (I) [0.667 and 0.333 (3)] are quite different from the occupancy factors (0.5) for the Ni atoms that are disordered by the mirror plane; it therefore seems likely that the order of the 15C5 rings is not closely tied to the order of the $H_2O-Ni-OH_2$ unit.

3.7. The modulation in phase (II)

Examination of Fig. 5 suggests that there is a modulation wave parallel to **c*** of the $P2_1$ cell, which is **a*** − **c*** of the $B2_1$ cell. This conclusion is consistent with the existence of streaks in those directions (see Fig. 6), which might indicate that the modulation wave is somewhat variable, at least at 90 K. Packing diagrams drawn with the program *Mercury* (Macrae *et al.*, 2008) show that the 2_1 axes (*e.g.* at the corners of the $P2_1$ and $B2_1$ cells) lie at the centers of the bands of more ordered residues (centered on the complex containing Ni_2) and the bands of less ordered residues (centered on the 15 C5_4 molecule).

4. Discussion

This compound provides another example (see Siegler, Hao *et al.*, 2011) of a phase sequence that includes an intermediate, high-Z' (or, more likely, incommensurate) phase [here, (II)] in which regions (here, slablike regions) that are like the phase stable at immediately higher temperatures [here, phase (I)] alternate with regions that are like the phase [here, (III)] stable at immediately lower temperatures. These alternating regions seem not to occur randomly, or to fluctuate with time, because there are diffraction maxima that correspond to a larger unit cell, which means that the modulated structure must be coherent over at least many nm. A description in terms of the condensation of a soft compression mode might be appropriate.

The related compound that gives such a set of phases, $[Ni(H_2O)_6](NO_3)_2\cdot$(15-crown-5)$\cdot 2H_2O$ (NiW6-2W; Siegler, Hao *et al.*, 2011) has layers similar to those in Ni-MeCN (see Figs. 5, 7 and 8) although in the NiW6-2W structure there are strong O—H···O hydrogen bonds within the layers containing the Ni complexes, which are cations. If flash-cooled from room temperature to 90 K both compounds 'get stuck' in the intermediate phase, which is metastable at 90 K. The identification of the phase metastable at 90 K as the intermediate, high-Z' phase stable in a higher temperature range is essentially certain in the case of NiW6-2W because the modulated structure could be refined near the low end (213 K) of its stability range. In the case of Ni-MeCN the identification depends on comparisons of the reconstructed reciprocal-lattice slices and on the analogy with the NiW6-2W system. Another important difference between the two systems is that the modulated NiW6-2W phase is stable over *ca* 40 K, while the modulated Ni-MeCN phase is stable over less than 10 K.

The Ni-MeCN system has four phases of which the modulated phase is the second found when a crystal is cooled; in the NiW6-2W it is the third phase that is modulated. The $[Ni(H_2O)_6]^{2+}$ cation can conform to a true twofold axis perpendicular to the hydrogen-bonded chain so that there is complete disorder of the 15C5 ring in the highest termperature phase (I) of NiW6-2W. Much of this disorder is resolved in phase (II) of NiW6-2W, but the disorder of the $H_2O-Ni-OH_2$ unit (and of C5/C6) in phase (II) of NiW6-2W is the same as in phase (I) of Ni-MeCN (see Fig. 10). In both systems it is the resolution of this $H_2O-Ni-OH_2$ disorder that takes place through the modulated phase. Resolution of the $H_2O-Ni-OH_2$ disorder leads to a completely ordered phase in NiW6-2W, but in Ni-MeCN there is residual *ap*/*sp* disorder of the κ^1O nitrato ligands. That residual disorder is resolved below the last transition.

Despite the similarities between the two systems their patterns of thermal contraction differ. In NiW6-2W (also refined in $B2_1$ rather than in group $P2_1$ so that the hydrogen-bonded chains would be along **c**) there is a discontinuous increase in the length *b* (the unique monoclinic axis) and a decrease in *a* as the $H_2O-Ni-OH_2$ disorder is resolved, but in the analogous transition in Ni-MeCN the length *b* drops and *a* increases discontinuously (see Fig. 9). In the description of the NiW6-2W phases (Siegler, Hao *et al.*, 2011) we suggested that the unusual phase behavior might be a consequence of the presence of alternating layers having very different intermolecular and interionic interactions. The same explanation might apply here, although the two kinds of layers in Ni-MeCN are less different than are the layers in NiW6-2W because in Ni-MeCN there are no ions and no strong intralayer hydrogen bonds. Another important difference between the two systems is the role in NiW6-2W of the hydrogen bond between the 'fifth' ether O atom and an equatorial water ligand; this bond occurs in the lowest temperature phase and in some regions of the modulated phase. That hydrogen bond favors alignment of the layers' 15C5 molecules and of Ni complexes. There is no analogy to that interaction in the Ni-MeCN system; there may be C—H···N interactions between the layers, but if so they are much weaker than the O—H···O bonds. The transition in the two systems into the modulated phase from above, however, does take place at about the same temperature (240–250 K).

We made rotatable overlays of phases (I) and (III) of Ni-MeCN and phases (II) and (IV) of NiW6-2W using the program *Mercury* (Macrae *et al.*, 2008) and then spent much time examining them in order to try to understand the transitions into and out of the modulated phases. We concluded that the transitions are much easier to describe than to understand. The differences between the Ni-MeCN phases are most easily seen in the planes shown in Figs. 7 and 8, but the modulation is not normal to those planes (see Fig. 5) and so must involve the interactions between the Ni complexes, the 15C5 molecules, and the lattice MeCN molecules. The modulations are better defined, and somewhat simpler, in NiW6-2W than in Ni-MeCN, but the wave direction in the former is more difficult to understand.

The existence of a high-Z' (or, more likely, incommensurate) intermediate phase suggests that the change between the two adjacent phases requires that one group of atoms move past another in some non-simple way. The anisotropy of the

thermal contraction during the transition (see Fig. 9) supports that idea. If so, however, the structural adjustments are so subtle that we were unable to identify them.

The lower-temperature transition (III) ↔ (IV) in Ni-MeCN is interesting because it is most obvious in the intensities of the $h0\ell$, ℓ odd reflections of phase (IV) (see Fig. 4). Difficulties with the refinements at temperatures at 140 and 130 K suggest that domains of (III) ($P2_1/c$) exist at temperatures (*ca* 145 K) below which the $h0\ell$, ℓ odd reflections start to have measurable intensities.

5. Summary

A study of $[Ni(MeCN)(H_2O)_2(NO_3)_2]\cdot$(15-crown-5)·MeCN (Ni-MeCN) in the range 90–273 K shows the details in the changes of the structure as the crystal passes through three phase transitions. Like crystals of the related compound $[Ni(H_2O)_6](NO_3)_2\ell$(15-crown-5)$\ell 2H_2O$ (NiW6-2W; Siegler, Hao *et al.*, 2011), crystals of Ni-MeCN pass through three phase transitions without loss of diffracting power. As in NiW6-2W one of the intermediate phases is a modulated (high-Z' or incommensurate) phase in which regions like those in the phase stable at somewhat higher temperatures alternate with regions like those in the phase stable at somewhat lower temperatures. In both compounds the conventional phases on either side of the modulated phase [(I) and (III) in the case of Ni-MeCN; (II) and (IV) in the case of NiW6-2W] are very similar, but disorder in the higher-T phase is resolved in the lower-T phase. The structural differences between phases (I) and (III) In Ni-MeCN, and between (II) and (IV) in NiW6-2W, could be identified, but the reasons for the transitions, and for the existence of the modulated phases have proved elusive.

M. A. Siegler thanks the University of Kentucky for a 2006–07 Kentucky Opportunity Fellowship. We thank Professor Mark D. Watson of the University of Kentucky Chemistry Department for help with the DSC measurements.

References

Allen, F. H. (2002). *Acta Cryst.* B**58**, 380–388.
Flack, H. D. (1983). *Acta Cryst.* A**39**, 876–881.
Macrae, C. F., Bruno, I. J., Chisholm, J. A., Edgington, P. R., McCabe, P., Pidcock, E., Rodriguez-Monge, L., Taylor, R., van de Streek, J. & Wood, P. A. (2008). *J. Appl. Cryst.* **41**, 466–470.
Nonius (1999). *Collect* and *DENZO-SMN*. Nonius BV, Madison, Wisconsin, USA.
Otwinowski, Z. & Minor, W. (2006). *International Tables for Crystallography*, Vol. F, ch. 11.4, pp. 226–235. Heidelberg: Springer.
Sheldrick, G. M. (2008). *Acta Cryst.* A**64**, 112–122.
Siegler, M. A., Hao, X., Parkin, S. & Brock, C. P. (2011). *Acta Cryst.* B**67**, 486–498.
Siegler, M. A., Parkin, S., Angel, R. J. & Brock, C. P. (2011). *Acta Cryst.* B**67**, 130–143.
Siegler, M. A., Parkin, S., Selegue, J. P. & Brock, C. P. (2008). *Acta Cryst.* B**64**, 725–737.
Siegler, M. A., Prewitt, J. H., Kelley, S. P., Parkin, S., Selegue, J. P. & Brock, C. P. (2010). *Acta Cryst.* B**66**, 213–221.